Au-329(SR)(84) Nanomolecules: Compositional Assignment of the 76.3 kDa Plasmonic Faradaurates

ARTICLE *in* ANALYTICAL CHEMISTRY · APRIL 2014

Impact Factor: 5.64 · DOI: 10.1021/ac403851s · Source: PubMed

2 AUTHORS:

Chanaka Kumara
University of Mississippi
20 PUBLICATIONS **307** CITATIONS

SEE PROFILE

Amala Dass
University of Mississippi
108 PUBLICATIONS **3,287** CITATIONS

SEE PROFILE

analytical chemistry

Article

pubs.acs.org/ac

$Au_{329}(SR)_{84}$ Nanomolecules: Compositional Assignment of the 76.3 kDa Plasmonic Faradaurates

Chanaka Kumara and Amala Dass*

Department of Chemistry and Biochemistry, University of Mississippi, University, Mississippi 38677, United States

Supporting Information

ABSTRACT: The purpose of this work is to determine the chemical composition of the previously reported faradaurates, which is a large 76.3 kDa thiolated gold nanomolecule. Electrospray ionization quadrupole-time-of-flight (ESI Q-TOF) mass spectrometry of the title compound using three different thiols yield the 329:84 gold to thiol compositional assignment. The purity of the title compound was checked by matrix-assisted laser desorption ionization-time-of-flight (MALDI-TOF) mass spectrometry. Positive and negative mode ESI-MS spectra show identical peaks denoting that there are no counterions, further reinforcing the accuracy of the assigned composition. We intentionally added Cs^+ ions to show that the $Au_{329}(SR)_{84}$ is the base molecular ion, with several Cs^+ adducts. A comprehensive investigation including analysis of the title compound with three ligands, in positive and negative mode and Cs^+ adduction, leads to a conclusive composition of $Au_{329}(SR)_{84}$. This formula determination will facilitate the fundamental understanding of emergence of surface plasmon resonance in $Au_{329}(SR)_{84}$ with 245 free electrons.

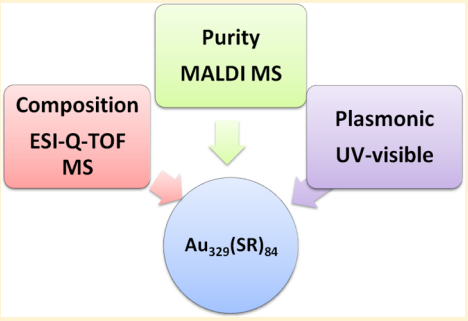

Gold nanomolecules are ultrasmall gold nanoparticles (<3 nm) with a precise number of metal atoms and organic thiolate groups.[1−3] They display interesting optical, magnetic, electrochemical properties with applications in catalysis, sensing, and biomedical devices. Typical examples include $Au_{25}(SR)_{18}$,[4] $Au_{38}(SR)_{24}$,[5] $Ag_{44}(SR)_{30}$,[6] $Au_{67}(SR)_{35}$,[7] and $Au_{144}(SR)_{60}$.[8] Recently, we reported a larger nanomolecule with 76.3 kDa, ∼2.0 nm in size, with ∼320 Au core atoms, which is the smallest Au nanoparticle to support plasmon resonance.[9] The objective of this work is to determine the elemental composition of the 76.3 kDa nanomolecule that is to establish a molecular formula of the form $Au_x(SR)_y$.

Mass spectrometry (MS) is the most common method to study the composition of gold nanomolecules.[10] This is due in part to (a) the ability to analyze mixture of products, (b) the ability to use commercially available mass spectrometers, and (c) the simple and robust nature of the sample preparation and analysis. Whetten's seminal report[11] in 1996 on laser desorption ionization (LDI)-MS of Au nanoparticles, partly inspired by MS of fullerenes,[12] provided conclusive information on the mass of the Au core, that is Au_x (where x is the number of gold atoms). However, the organic ligands underwent extensive fragmentation, thus hindering full compositional assignment of the form $Au_x(SR)_y$, where y is number of ligands attached. Murray's group in 2007 reported two major advances[13,14] in nanoparticles MS that transformed the field by facilitating the formation and detection of fully intact molecular nanoparticle ions. The first advance deals with electrospraying[13] molecular ions in an organic solvent, with and without the presence of counterions such as Cs^+. The second deals with the generation of intact ions in matrix-assisted laser desorption ionization-time-of-flight (MALDI-TOF)[14] using the aprotic DCTB matrix. Together these two methods, with minimal modification, account for the majority of today's nanoparticle literature worldwide for intact nanoparticle identification. We and others have successfully applied MS methods, including MALDI, electrospary ionization (ESI), and fast atom bombardment (FAB) ionization, to study the synthesis,[15−17] ligand exchange,[18−20] dithiol cross-linking,[21] fragmentation pattern,[22] ion-mobility MS,[22,23] and identity of several gold,[5,7,9,24−26] silver,[6,27] and Au-metal alloy[28−32] nanomolecules.

As the size of the nanomolecule increases, the ionization and detection of intact molecular ions become increasingly difficult. The large size, in addition to issues of adduct formation due to counterions makes the assignment of larger (>200 atom, >40 kDa) nanomolecules nontrivial. Therefore, in our recent work[9] in 2011, we simply identified the faradaurates, which is a plasmonic nanomolecule, as having a mass of 76.3 kDa. In early 2012, Jin's group independently reported[33] a nanoparticle of nearly identical mass, ∼76 kDa. On the basis of ESI experiments performed in the presence of cesium acetate salt, they assigned its composition as $Au_{333}(SCH_2CH_2Ph)_{79}$.

Here, we use high-resolution ESI-Q-TOF MS to obtain the composition of the 76.3 kDa nanomolecules (Scheme 1). By synthesizing this nanomolecule with three different thiols, we obtain the $Au_{329}(SR)_{84}$ composition. Positive and negative mode analysis of title samples show absence of counterions.

Received: November 27, 2013
Accepted: February 28, 2014

   dx.doi.org/10.1021/ac403851s | *Anal. Chem.* XXXX, XXX, XXX−XXX

Scheme 1. Compositional Determination and Mass Spectrometric Methods Used in This Study

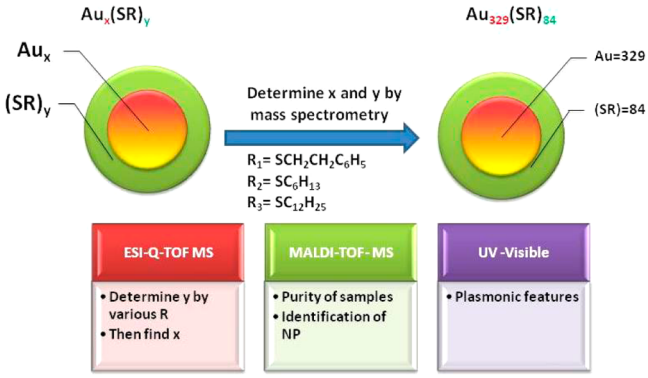

The deconvolution of several charge states all agree with the 329:84 composition.

MATERIALS AND METHODS

Materials. Sodium borohydride (Acros, 99%), phenylethanemercaptan (SAFC, ≥99%), and *trans*-2-[3[(4-tertbutylphenyl)-2-methyl-2-propenylidene]malononitrile (DCTB matrix) (Fluka ≥99%) were purchased from Aldrich. HPLC grade solvents such as toluene, methanol, acetone, and acetonitrile were obtained from Fisher Scientific.

Methods. *Synthesis.* Synthesis of the $Au_{329}(SR)_{84}$ involves three steps. The first step is the synthesis of crude product that contains polydisperse gold particles according to a modified version of our recent report.[9] The second step is the thermochemical treatment of the crude product with excess thiol to remove meta-stable clusters. The final step is the solvent fractionation to isolate 76.3 kDa nanomolecules. Briefly, an aqueous solution (30 mL) containing $HAuCl_4$ (0.9 mmol/0.3566 g) was mixed with a toluene solution (30 mL) of tetraoctylammonium bromide, TOABr (1.1 mmol/0.6050 g). After stirring for 30 min, the organic phase was separated and phenylethane thiol (0.90 mmol) was added and further stirred for 30 min at room temperature (gold to thiol molar ratio was set to 1:1). Note that the 1:1 Au to thiol ratio is important in the formation of the 76.3 kDa species. The 1:1 ratio is different than the commonly used 1:3 Au to thiol ratio to prepare smaller <200 atom nanomolecules. This solution was cooled in an ice bath for 30 min. An aqueous solution of $NaBH_4$ (20 mmol, 20 mL) cooled to 0 °C was rapidly added to the reaction mixture under vigorous stirring. After 3 h, the organic layer was separated and evaporated to dryness. The product was washed with methanol to remove other byproducts. The residual mixture was extracted with toluene. Then, ∼100 mg of crude products was dissolved in 1 mL of toluene and subjected to thermochemical treatment with excess phenylethanethiol (1 mL) at 80 °C under stirring, while monitoring with MALDI MS (see Figure S2 in the Supporting Information). After the metastable clusters disappeared (∼8 days), the thermochemical treatment was discontinued and the product mixture was washed with methanol several times. Finally, the product was dissolved in toluene and subjected to solvent fractionation with a toluene/MeOH mixture to isolate the pure 76.3 kDa nanomolecules (see Figure S3 in the Supporting Information).

Analysis. MALDI mass spectra were acquired with a Bruker Daltonics Autoflex 1 mass spectrometer using DCTB matrix[14] at optimal laser fluence. At least 500 individual spectra were collected and averaged for MALDI-MS, and spectral analyses were done using Bruker Daltonics flexAnalysis version 3.0. ESI mass spectra were obtained from a Waters Synapt HDMS in 50:50 toluene−CH_3CN or 50:50 THF−CH_3CN solvent mixture. ESI-MS spectra were collected over a 5 min time period and averaged to acquired data with best possible signal-to-noise ratio. Calibration check was performed with $Au_{25}(SCH_2CH_2Ph)_{18}$ and $Au_{144}(SCH_2CH_2Ph)_{60}$. UV−visible−NIR spectra were recorded in toluene solutions using a Shimadzu UV-1601 spectrophotometer/UV probe 2.0 software in the 300−1100 nm range.

RESULTS AND DISCUSSION

Figure 1 shows the MALDI-TOF mass spectrum of the 76.3 kDa nanomolecule. There is a broad peak centered at ∼76 kDa

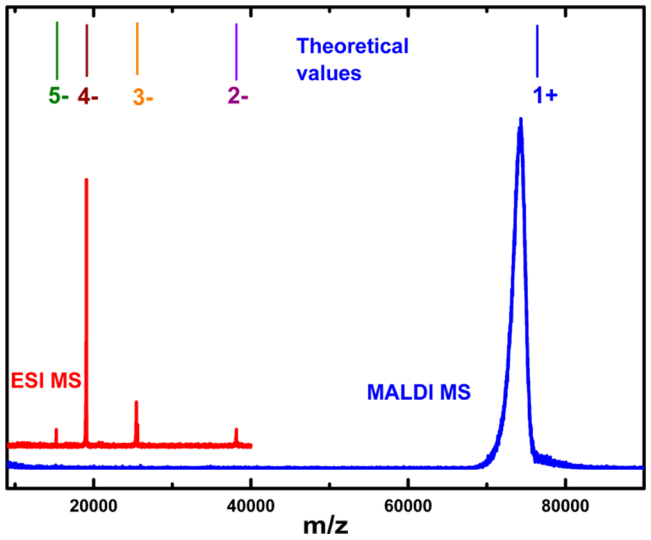

Figure 1. ESI-MS (red) and MALDI-MS (blue) spectra of 76.3 kDa nanomolecules synthesized using $HSCH_2CH_2C_6H_5$ thiol. The lines at the top indicate the theoretical values for the 1, 2, 3, 4, and 5 charge states of $Au_{329}(SCH_2CH_2Ph)_{84}$.

corresponding to the 1+ molecular ion. The features are broad due to the inherent resolution limitations of the linear TOF tube in the MALDI instrument. ESI Q-TOF MS of the samples showed multiply charged peaks at 38, 25, 19, and 15 kDa/z corresponding to 2−, 3−, 4−, and 5− ions, respectively. Then deconvolution of the 2−, 3−, 4− and 5− peaks all point consistently to the 76.3 kDa molecular ion. The MALDI and ESI data were reported in our previous communication[9] but are presented here for completeness and clarity and because it is foundational for understanding this work.

Composition by Varying the Mass of the Ligand. An independent method to determine the chemical composition involves the mass spectrometric measurement of the same nanomolecule with different stabilizing organic thiols. It is now generally recognized that for many stable nanomolecules, the same fixed composition $[Au_x(SR)_y]$ is obtained even when different thiol groups are used in the synthesis.[7,25,34] For example, the $Au_{25}(SR)_{18}$, $Au_{38}(SR)_{24}$, $Au_{67}(SR)_{35}$ and $Au_{144}(SR)_{60}$ are obtained when the R group is varied to either $-SCH_2CH_2Ph$, $-SC_6H_{13}$ or $-SC_{12}H_{25}$. Therefore, if the same nanomolecule $Au_x(SR)_y$ is obtained using two different thiols, one can determine the number of ligands, y. From y, one can

dx.doi.org/10.1021/ac403851s | *Anal. Chem.* XXXX, XXX, XXX−XXX

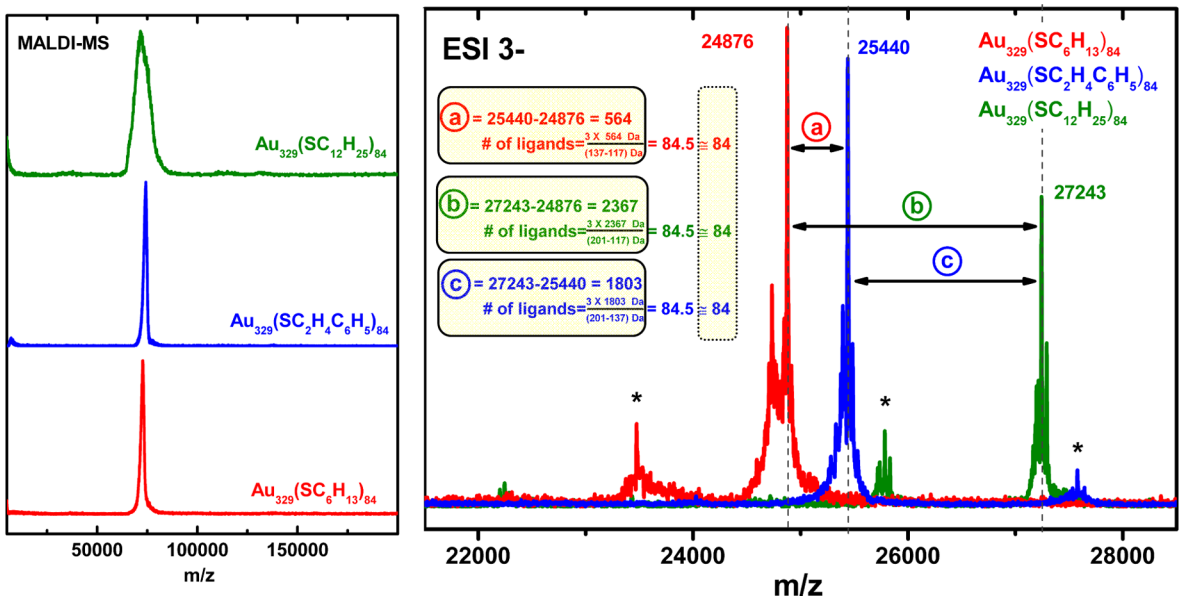

Figure 2. Ligand count determination by analyzing 76.3 kDa species protected by various ligands. (Left) MALDI-MS of the 76.3 kDa nanomolecule synthesized using dodecanethiol (olive), phenylethanethiol (blue), and hexanethiol (red). (Right) ESI-MS Q-TOF of 3- ions of the 76.3 kDa nanomolecules using three ligands. Assuming that the number of metal atoms is constant, for the 76.3 kDa nanomolecule for these three ligands (as in the case of $Au_{25}(SR)_{18}$, $Au_{38}(SR)_{24}$ and $Au_{144}(SR)_{60}$), the number of ligands is calculated by the mass difference of the intact ESI ions. The ligand count was found to be 84 in all cases, which then leads to the Au atom count of 329 atoms. Peaks marked by an asterisk indicate remaining impurities not removed during purification or other minor species present in the sample. Dotted lines indicate the theoretical mass of the 3− ions of corresponding $Au_{329}(SR)_{84}$ nanomolecules. The mass error of the 3− ions of the nanoparticles synthesized using hexanethiol, phenylethanethiol, and dodecanethiol was found to be 341, 118, and 96 ppm, respectively.

determine the number of Au atoms, *x*, leading to the full elemental composition, $Au_x(SR)_y$.

The title nanomolecule was prepared using one of the three thiols each, namely, $-SCH_2CH_2Ph$ (137 Da), $-SC_6H_{13}$ (117 Da), or $-SC_{12}H_{25}$ (201 Da). Figure 2 (left) shows the MALDI mass spectrum of these nanomolecules. All three MALDI spectra show one peak in the ∼75 kDa region, corresponding to the 1+ molecular ion, indicating the purity of the sample. MALDI spectra show broad features when compared to the ESI mass spectrometry. This is due to the laser induced fragmentation occurring during the ionization process. This involves possible Au−S or S−C bond breaking within the $Au_{329}(SR)_{84}$ nanomolecules. We note that the $-SC_{12}H_{25}$ spectra on top actually shows a lower mass peak than other ligands, even though this is supposed to be heavier in mass. This is due to the significant chemical differences between the three ligands. More specifically, the intermolecular interactions are dramatically enhanced in the long chain $SC_{12}H_{25}$ ligand. This is distinctly manifested during the synthesis and processing of the $-SC_{12}H_{25}$ protected title compound. The dodecanethiol ligand is waxy and very difficult to purify and process. This is also the reason why we could not manage to obtain a very pure title material using this ligand as seen in Figure S5 in the Supporting Information. We believe that this intermolecular interaction and the waxy nature of the ligand significantly affects the matrix assisted laser desorption ionization process. It is likely that we used relatively higher laser intensity to ionize this sample. This is the reason for the unusually broad feature for the MALDI spectra of the $Au_{329}(SC_{12}H_{25})_{84}$ nanomolecules. Therefore, ESI-MS were recorded to determine the mass of the intact molecular ions without fragmenting.

Figure 2 (right) also shows the expansion of the 3− ions for ESI-MS of the title compound with the three thiols. From the mass difference of the three nanomolecules and the mass difference of the ligand, the number of ligands, *y*, can be calculated. The number of ligands was calculated to be "84" using the three independent mass differences *a*, *b*, and *c*, as shown in Figure 2. From the value of $y = 84$, the number of Au atoms, *x*, was found to be 329. Note that there are many literature precedents for using the difference in mass of ligands to accurately determine the compositional assignment.[7,25] Many of these reports are independently verified later by complementary techniques such as thermogravimetric analysis, X-ray crystallography, and optical spectroscopy.

The full range ESI-MS spectra of nanomolecules synthesized using the three different thiols are shown in Figure S5 in the Supporting Information. The spectra of the $Au_{329}(SC_6H_{13})_{84}$ and $Au_{329}(SC_{12}H_{25})_{84}$ have the 3− charge ions as the dominating species, whereas the 4−/+ charge species are dominant in $Au_{329}(SCH_2CH_2C_6H_5)_{84}$ nanomolecules. For hexanethiol protected $Au_{329}(SC_6H_{13})_{84}$ nanomolecules, the 4−/+ charge ions were hardly observed. Therefore, considering the signal of all three nanomolecules, the 3− ions were chosen for the compositional assignment in Figure 2 (right).

Significant efforts were made to assign the ESI-MS peaks that are at lower mass than the principal peaks. The minor peak to the right of the title compound is closely related to the $Au_{329}(SC_2H_4C_6H_5)_{85}$ assignment, and the peak to the left of the title compound is closely related with the assignment $Au_{328}(SC_2H_4C_6H_5)_{84}$.

Other lower mass peaks are less pronounced and were not observed repeatedly in the samples that were synthesized using three different thiols and in both positive and negative mode. Because of the low signal intensity and the lack of reproducible

dx.doi.org/10.1021/ac403851s | *Anal. Chem.* XXXX, XXX, XXX−XXX

observation of these peaks, it was not possible to assign these minor species. For smaller nanoparticles like $Au_{25}(SR)_{18}$ and $Au_{38}(SR)_{24}$, there exists only one main species. However for larger nanoparticles, such as Au_{144}, there are reports on many closely related species such as $Au_{144}(SR)_{59}$, $Au_{144}(SR)_{60}$, $Au_{146}(SR)_{59}$, etc. However $Au_{144}(SR)_{60}$ is the dominant species, and the others are present in very small amounts (<10%). Negishi showed that the existence of several possible configurations with the thiol protected $Au_{130}(SR)_{50}$ and $Au_{187}(SR)_{68}$ nanomolecules based on mass spectrometric analysis.[25] On the basis of these previous observation on other sizes, it is possible to have many closely related species for the title compound in the 76.3 kDa range. Fragmentation or dissociative species were not observed in the control ESI-MS spectra of $Au_{144}(SC_2H_4C_6H_5)_{60}$ under the same experimental conditions (see Figure S4 in the Supporting Information).

Interference from Adducts, Cations, and Anions. Easily misinterpreted mass spectral adduct peaks frequently arise due to the sum of the molecular ion of interest plus some counterion. For example, $Au_{25}(SCH_2CH_2Ph)_{18}^-$ shows a peak at 7394 Da in the negative mode corresponding to the singly charged negative ion, $Au_{25}(SCH_2CH_2Ph)_{18}^-$. However the same sample in the positive mode yields a peak at 8326 Da, corresponding to $[Au_{25}(SCH_2CH_2Ph)_{18}\cdot 2(N(C_8H_{17})_4)\ ]^+$. This is because the molecular ion with two tetraoctylammonium cations results in an adduct, whose overall charge is 1+. So it is critical (but often ignored in nanoparticle MS literature) to obtain the mass spectrum in both positive and negative mode to *check for counterions and adduct formation*.

Figure 3a shows the title nanomolecule in both positive and negative mode. Figure 3b shows the expansion of the 4−/+ region. Based on Figure 3, it is made clear that both positive and negative mode shows peaks at the same mass of 19.079 kDa. This suggests that the entire mass in the 19.079 kDa peak corresponds to Au atoms and organic ligands, and the absence of counterions or adducts like $N(C_8H_{17})_4^+$, Cs^+, or Na^+. Despite the adduct formation in $Au_{25}(SR)_{18}$, larger nanoparticles such as Au_{67} and Au_{144} show peaks in the same mass in both positive and negative modes (see ref 7 and see Figure S4 in the Supporting Information). The observation of ions at identical mass in both positive and negative mode for the title nanomolecule confirms that the entire mass of 19.079 kDa peak is due to only Au atoms and SR organic ligands. Hence the $Au_{329}(SR)_{84}$ assignment is not affected by counterions such as $N(C_8H_{17})_4^+$, Cs^+, or Na^+.

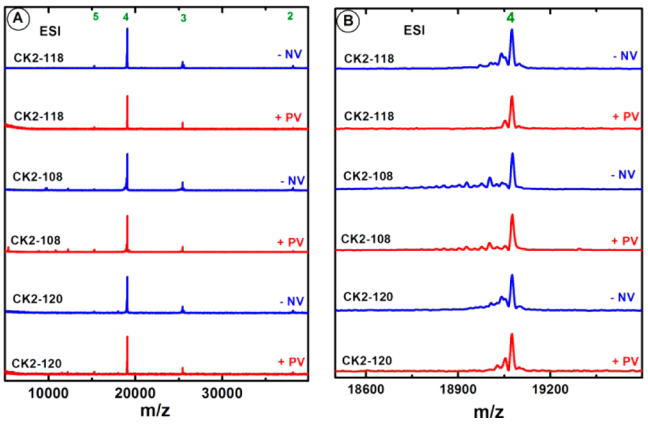

Figure 3. (A) Positive (red) and negative (blue) mode ESI Q-TOF mass spectra of $Au_{329}(SCH_2CH_2C_6H_5)_{84}$ nanomolecules of three different synthetic batches (CK2-118, CK2-108, and CK2-120). (B) Expansion of the 4−/+ ESI peak region of $Au_{329}(SCH_2CH_2C_6H_5)_{84}$. The spectra shows that all the samples in both positive and negative mode show the same 4−/+ peak at 19 079 Da, denoting the absence of adducts (counterions, Na^+ or Cs^+ ions).

We also show the positive and negative mode ESI spectra of three different synthetic batches (CK2-118, CK2-108, CK2-120), giving a total of six representative spectra. These six spectra (including a total of 10 different synthetic batches, not shown here, by two different researchers), all agree with the $Au_{329}(SR)_{84}$ assignment and point toward the reproducibility of the data (see Table S1 in the Supporting Information).

Figure 4 shows the deconvoluted spectra of 2−/+, 3−/+, 4−/+, and 5−/+ ions to the 1−/+ molecular ion (refer to Figure S6 in the Supporting Information for the deconvolution process). The good match among these peaks in agreement with the $Au_{329}(SR)_{84}$ assignment adds confidence to the composition. The variation in the signal-to-noise ratio is due to the signal intensity variation at various mass ranges of the multiply charged peaks. In particular, the lower signal/noise for 2−/+ and 5−/+ peaks is due to the low signal for these peaks in the original spectrum. The title compound is observed predominantly as 4−/+ ions, with the 3−/+ ions being the next intense peak (see Figure 1 for an example).

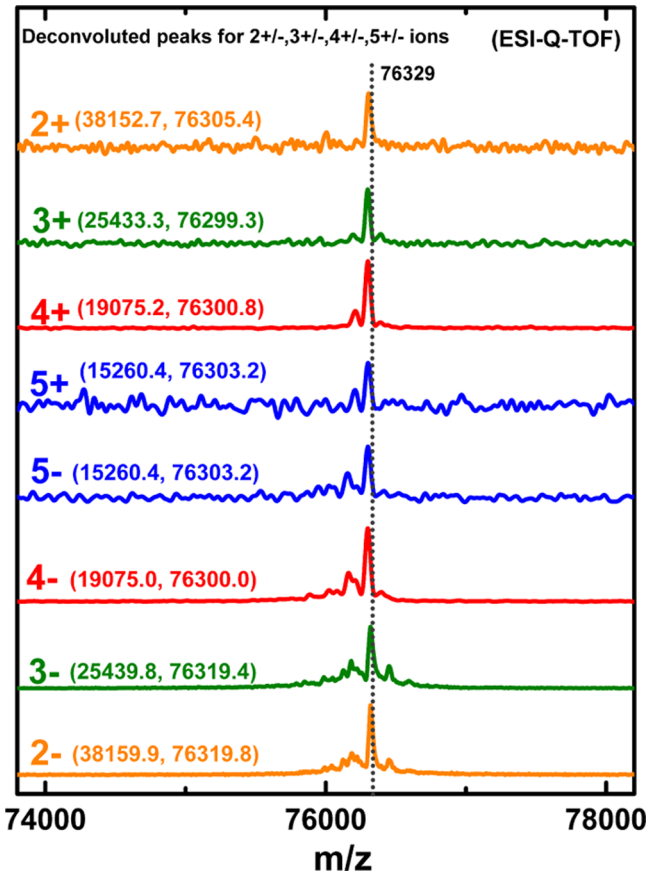

Figure 4. Deconvolution of 2−, 3−, 4−, 5−, 2+, 3+, 4+ and 5+ ions to the corresponding 1−/+ molecular ions, adding confidence to the $Au_{329}(SCH_2CH_2C_6H_5)_{84}$ assignment (the number in the parentheses represent the m/z values of the particular multiply charged species and it's deconvoluted mass value). The dotted line shows the theoretical value (76 329 Da) of the $Au_{329}(SCH_2CH_2C_6H_5)_{84}$ nanomolecules.

dx.doi.org/10.1021/ac403851s | *Anal. Chem.* XXXX, XXX, XXX−XXX

Cesium acetate is commonly added to nanoparticle mass spectrometric analyses to facilitate the formation of ions by Cs^+ adduction. This was first reported by the Murray group, where Li^+, Na^+, Rb^+, and Cs^+ adducts of $Au_{25}(SCH_2CH_2Ph)_{18}$ were observed in ESI-MS.[35] In general, an envelope of nanoparticles corresponding to $Au_{25}(SR)_{18}{\cdot}nCs^+$ where n = 0, 1, 2, 3 can be observed. Subsequently, Cs^+ adducts of other nanoparticles that were not easily ionized in their native state were reported.[36,37,33] The Cs^+ adduction improves the signal by enhancing ionization and works well for previously known, or well studied species.[36,37] Nevertheless, applying this to a new nanomolecule with previously unknown composition can be complicated due to the difficulty in identifying the molecular ion without any cesium. Therefore, in this study, we have not used cesium acetate or other species that is routinely used to promote ionization.

To compare with other literature work, we intentionally added cesium to one mass spectrometry analysis to show that cesium adduction can be observed. We observed (see Figure 5) an envelope of peaks corresponding to $Au_{329}(SR)_{84}{\cdot}nCs^+$, where n = 0, 1, 2, and 3 . The addition of more cesium completely shifts the envelope to even higher mass. Table S2 in the Supporting Information shows the comparison between experimental and theoretical m/z values of the Cs addition experiments further confirming the assignment 329:84. Table S3 in the Supporting Information summarized the possible Au and ligand combination for the 76 kDa nanomolecules. Both mass difference method and Cs^+ addition experiment shows the formula to be 329:84.

Another report on a similar sized plasmonic nanoparticle has assigned this nanoparticle to $Au_{333}(SCH_2CH_2Ph)_{79}{\cdot}nCs^+$, using cesium acetate to promote ionization.[33] This results in an envelope of peaks as expected with many cesium adducts. If the number of cesium ions is not accurately assigned, then the ions with Cs+ adduct can lead to erroneous assignment. The low signal-to-noise ratio peak corresponding to $Au_{333}(SCH_2CH_2Ph)_{79}$ in ref 33 is a decent match with the composition reported here, namely, $Au_{329}(SCH_2CH_2Ph)_{84}{\cdot}1Cs^+$. It remains to be seen if the work in ref 33 can be reproduced without Cs+ ions and obtain the same $Au_{333}(SCH_2CH_2Ph)_{79}$ composition. This will help in determining if there are two closely related species, namely, $Au_{329}(SR)_{84}$ and $Au_{333}(SR)_{79}$, or if the $Au_{333}(SR)_{79}$ composition needs to be corrected to properly account for the number of Cs+ ions.

Optical Properties. The UV−visible−NIR spectra of $Au_{329}(SR)_{84}$ nanomolecules synthesized using three different thiols (R groups) shows plasmonic band at around 495 nm (see Figure 6). For a neutral charge state, the number of free electrons was calculated to be 245 (329 − 84). There must be a threshold number of free electrons before the surface plasmon resonance (SPR) can be supported due to the collective

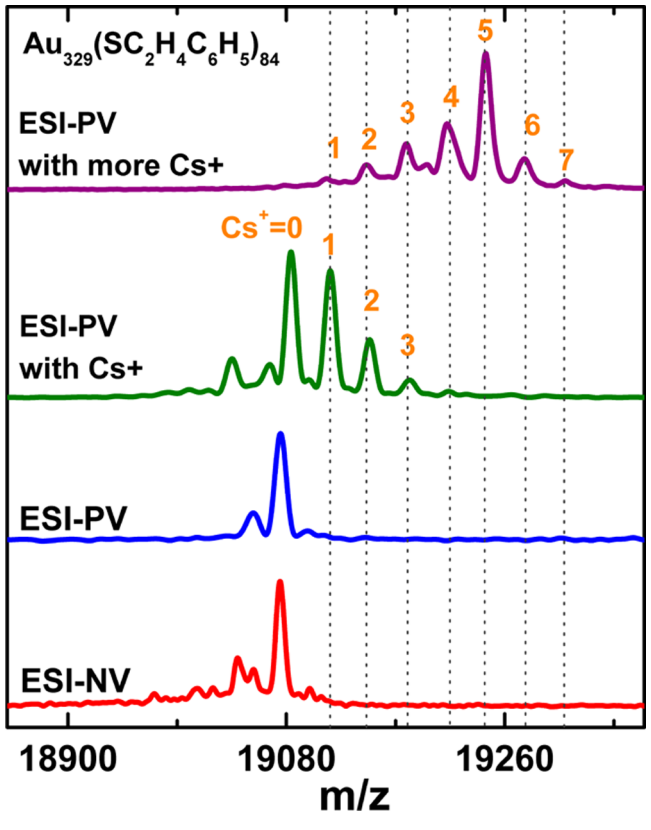

Figure 5. $Au_{329}(SCH_2CH_2C_6H_5)_{84}$ with negative mode (NV, red) and positive mode (PV, blue) in the presence of cesium acetate (PV, olive) and further addition of cesium acetate (PV, purple) . The positive and negative spectra shows the 4+ and 4− molecular ions, respectively, while the addition of cesium acetate leads additional peaks due to the formation of Cs+ adducts, such as $Au_{329}(SCH_2CH_2C_6H_5)_{84}{\cdot}Cs^+$, $Au_{329}(SCH_2CH_2C_6H_5)_{84}{\cdot}2Cs^+$, $Au_{329}(SCH_2CH_2C_6H_5)_{84}{\cdot}3Cs^+$. Further addition of cesium acetate leads to adducts with 4, 5, 6, and 7 Cs^+ ions.

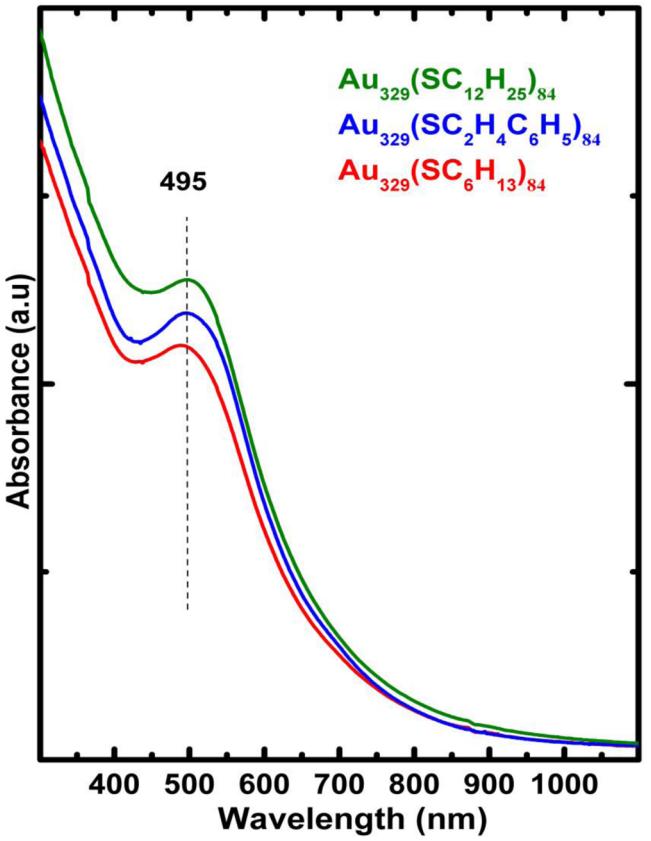

Figure 6. UV−visible−NIR spectra of $Au_{329}(SR)_{84}$ nanomolecules synthesized using dodecanethiol (olive), phenylethanethiol (blue), and hexanethiol (red). All three spectra show the SPR peak. The 329-atom is the smallest $Au_n(SR)_m$ nanomolecule that supports a surface plasmon resonance. The emergence of SPR peak in 329-atom compared with $Au_{144}(SR)_{60}$ is shown in ref 9.

dx.doi.org/10.1021/ac403851s | Anal. Chem. XXXX, XXX, XXX−XXX

oscillation of conduction electrons. This threshold value is apparently reached or exceeded at 245 free electron count and may be crucial in determining if a certain size would support SPR. The optical spectra of smaller nanomolecules, $Au_{144}(SR)_{60}$ and $Au_{187}(SR)_{68}$, show discrete electronic states, having 84 and 119 free electrons, respectively. The newly determined 329:84 formula reveals that 245 free electrons are adequate to interact with incident radiation to support surface plasmon resonance. This is of great interest in fundamental understanding of plasmon emergence,[38] which has many applications.

CONCLUSION AND OUTLOOK

We report the composition of the 76.3 kDa plasmonic faradaurates to be $Au_{329}(SR)_{84}$ based on high-resolution mass spectrometric studies. This conclusion is supported by multiple independent and complementary lines of evidence including ionization mode switching and analysis of the mass shifts caused by changing the mass of the ligands. We anticipate that the composition reported here will facilitate the prediction of atomic structure and other theoretical and experimental studies to understand the properties of this extraordinarily stable plasmonic $Au_{329}(SR)_{84}$ nanomolecules.

ASSOCIATED CONTENT

Supporting Information

Additional information as noted in text. This material is available free of charge via the Internet at http://pubs.acs.org.

AUTHOR INFORMATION

Corresponding Author

*E-mail: amal@olemiss.edu.

Notes

The authors declare no competing financial interest.

ACKNOWLEDGMENTS

This material is based upon work supported by the NSF Grant CHE-1255519. We thank the reviewer of ref 9 who suggested to not assign the 76 kDa nanomolecule until the composition can be obtained with high confidence. We thank Santosh G. Valeja, Nathan K. Kaiser, Alan G. Marshall, and Nicholas L. Young for preliminary results and discussions.

REFERENCES

(1) Maity, P.; Xie, S.; Yamauchi, M.; Tsukuda, T. *Nanoscale* **2012**, *4*, 4027−4037.
(2) Wang, L.-M.; Wang, L.-S. *Nanoscale* **2012**, *4*, 4038−4053.
(3) Dass, A. *Nanoscale* **2012**, *4*, 2260−2263.
(4) Heaven, M. W.; Dass, A.; White, P. S.; Holt, K. M.; Murray, R. W. *J. Am. Chem. Soc.* **2008**, *130*, 3754−3755.
(5) Chaki, N. K.; Negishi, Y.; Tsunoyama, H.; Shichibu, Y.; Tsukuda, T. *J. Am. Chem. Soc.* **2008**, *130*, 8608−8610.
(6) Harkness, K. M.; Tang, Y.; Dass, A.; Pan, J.; Kothalawala, N.; Reddy, V. J.; Cliffel, D. E.; Demeler, B.; Stellacci, F.; Bakr, O. M.; McLean, J. A. *Nanoscale* **2012**, *4*, 4269−4274.
(7) Nimmala, P. R.; Yoon, B.; Whetten, R. L.; Landman, U.; Dass, A. *J. Phys. Chem. A* **2013**, *117*, 504−517.
(8) Lopez-Acevedo, O.; Akola, J.; Whetten, R. L.; Grönbeck, H.; Häkkinen, H. J. *J. Phys. Chem. C* **2009**, *113*, 5035−5038.
(9) Dass, A. *J. Am. Chem. Soc.* **2011**, *133*, 19259−19261.
(10) Harkness, K. M.; Cliffel, D. E.; McLean, J. A. *Analyst* **2010**, *135*, 868−874.
(11) Whetten, R. L.; Khoury, J. T.; Alvarez, M. M.; Murthy, S.; Vezmar, I.; Wang, Z. L.; Stephens, P. W.; Cleveland, C. L.; Luedtke, W. D.; Landman, U. *Adv. Mater.* **1996**, *8*, 428−433.
(12) Diederich, F.; Ettl, R.; Rubin, Y.; Whetten, R. L.; Beck, R.; Alvarez, M.; Anz, S.; Sensharma, D.; Wudl, F.; Khemani, K. C.; Koch, A. *Science* **1991**, *252*, 548−551.
(13) Tracy, J. B.; Kalyuzhny, G.; Crowe, M. C.; Balasubramanian, R.; Choi, J. P.; Murray, R. W. *J. Am. Chem. Soc.* **2007**, *129*, 6706−6707.
(14) Dass, A.; Stevenson, A.; Dubay, G. R.; Tracy, J. B.; Murray, R. W. *J. Am. Chem. Soc.* **2008**, *130*, 5940−5946.
(15) Dharmaratne, A. C.; Krick, T.; Dass, A. *J. Am. Chem. Soc.* **2009**, *131*, 13604−13605.
(16) Gies, A. P.; Hercules, D. M.; Gerdon, A. E.; Cliffel, D. E. *J. Am. Chem. Soc.* **2007**, *129*, 1095−1104.
(17) Zhang, Y.; Shuang, S.; Dong, C.; Lo, C. K.; Paau, M. C.; Choi, M. M. F. *Anal. Chem.* **2009**, *81*, 1676−1685.
(18) Knoppe, S.; Dharmaratne, A. C.; Schreiner, E.; Dass, A.; Bürgi, T. *J. Am. Chem. Soc.* **2010**, *132*, 16783−16789.
(19) Dass, A.; Holt, K.; Parker, J. F.; Feldberg, S. W.; Murray, R. W. *J. Phys. Chem. C* **2008**, *112*, 20276−20283.
(20) Shibu, E. S.; Muhammed, M. A. H.; Tsukuda, T.; Pradeep, T. *J. Phys. Chem. C* **2008**, *112*, 12168−12176.
(21) Jupally, V. R.; Kota, R.; Dornshuld, E. V.; Mattern, D. L.; Tschumper, G. S.; Jiang, D.-e.; Dass, A. *J. Am. Chem. Soc.* **2011**, *133*, 20258−20266.
(22) Angel, L. A.; Majors, L. T.; Dharmaratne, A. C.; Dass, A. *ACS Nano* **2010**, *4*, 4691−4700.
(23) Harkness, K. M.; Fenn, L. S.; Cliffel, D. E.; McLean, J. A. *Anal. Chem.* **2010**, *82*, 3061−3066.
(24) Nimmala, P. R.; Dass, A. *J. Am. Chem. Soc.* **2011**, *133*, 9175−9177.
(25) Negishi, Y.; Sakamoto, C.; Ohyama, T.; Tsukuda, T. *J. Phys. Chem. Lett.* **2012**, *3*, 1624−1628.
(26) Tsunoyama, R.; Tsunoyama, H.; Pannopard, P.; Limtrakul, J.; Tsukuda, T. *J. Phys. Chem. C* **2010**, *114*, 16004−16009.
(27) Abdul Halim, L. G.; Ashraf, S.; Katsiev, K.; Kirmani, A. R.; Kothalawala, N.; Anjum, D. H.; Abbas, S.; Amassian, A.; Stellacci, F.; Dass, A.; Hussain, I.; Bakr, O. M. *J. Mater. Chem. A* **2013**, *1*, 10148−10154.
(28) Kumara, C.; Dass, A. *Nanoscale* **2012**, *4*, 4084−4086.
(29) Kumara, C.; Dass, A. *Nanoscale* **2011**, 3064−3067.
(30) Negishi, Y.; Igarashi, K.; Munakata, K.; Ohgake, W.; Nobusada, K. *Chem. Commun.* **2012**, *48*, 660−662.
(31) Negishi, Y.; Iwai, T.; Ide, M. *Chem. Commun.* **2010**, *46*, 4713−4715.
(32) Fields-Zinna, C. A.; Crowe, M. C.; Dass, A.; Weaver, J. E. F.; Murray, R. W. *Langmuir* **2009**, *25*, 7704−7710.
(33) Qian, H.; Zhu, Y.; Jin, R. *Proc. Natl. Acad. Sci. U.S.A.* **2012**, *109*, 696−700.
(34) Stellwagen, D.; Weber, A.; Bovenkamp, G. L.; Jin, R.; Bitter, J. H.; Kumar, C. S. S. R. *RSC Adv.* **2012**, *2*, 2276−2283.
(35) Tracy, J. B.; Crowe, M. C.; Parker, J. F.; Hampe, O.; Fields-Zinna, C. A.; Dass, A.; Murray, R. W. *J. Am. Chem. Soc.* **2007**, *129*, 16209−16215.
(36) Qian, H.; Zhu, M.; Andersen, U. N.; Jin, R. *J. Phys. Chem. A* **2009**, *113*, 4281−4284.
(37) Qian, H.; Jin, R. *Nano Lett.* **2009**, *9*, 4083−4087.
(38) Malola, S.; Lehtovaara, L.; Enkovaara, J.; Häkkinen, H. *ACS Nano* **2013**, *7*, 10263−10270.